

# Distributed Rate-Splitting Multiple Access for Multilayer Satellite Communications

Yunnuo Xu, Longfei Yin, *Student Member, IEEE*, Yijie Mao, *Member, IEEE*,  
Wonjae Shin, *Senior Member, IEEE* and Bruno Clerckx, *Fellow, IEEE*

## Abstract

Future wireless networks, in particular, 5G and beyond, are anticipated to deploy dense Low Earth Orbit (LEO) satellites to provide global coverage and broadband connectivity with reliable data services. However, new challenges for interference management have to be tackled due to the large scale of dense LEO satellite networks. Rate-Splitting Multiple Access (RSMA), widely studied in terrestrial communication systems and Geostationary Orbit (GEO) satellite networks, has emerged as a novel, general, and powerful framework for interference management and multiple access strategies for future wireless networks. In this paper, we propose a multilayer interference management scheme for spectrum sharing in heterogeneous GEO and LEO satellite networks, where RSMA is implemented distributedly at GEO and LEO satellites, namely Distributed-RSMA (D-RSMA), to mitigate the interference and boost the user fairness of the system. We study the problem of jointly optimizing the GEO/LEO precoders and message splits to maximize the minimum rate among User Terminals (UTs) subject to a transmit power constraint at all satellites. A Semi-Definite Programming (SDP)-based algorithm is proposed to solve the original non-convex optimization problem. Numerical results demonstrate the effectiveness and robustness towards network load of our proposed D-RSMA scheme for multilayer satellite networks. Because of the data sharing and the interference management capability, D-RSMA provides significant max-min fairness performance gains when compared to several benchmark schemes.

## Index Terms

RSMA, max-min fairness, GEO, LEO, beamforming design, satellite communication

Y. Xu and L. Yin are with the Communications and Signal Processing Group, Department of Electrical and Electronic Engineering, Imperial College London, London SW7 2AZ, U.K. (email: yunnuo.xu19, longfei.yin17@imperial.ac.uk).

Y. Mao is with the School of Information Science and Technology, ShanghaiTech University, Shanghai 201210, China (email: maoyj@shanghaitech.edu.cn).

W. Shin is with the Department of Electrical and Computer Engineering, Ajou University, Suwon 16499, South Korea (email: wjshin@ajou.ac.kr).

B. Clerckx is with the Department of Electrical and Electronic Engineering at Imperial College London, London SW7 2AZ, UK and with Silicon Austria Labs (SAL), Graz A-8010, Austria (email: b.clerckx@imperial.ac.uk).

## I. INTRODUCTION

Low Earth Orbit (LEO) satellite is envisioned as an appealing method to support and enhance 5G New Radio (NR) and beyond-5G communications [1]–[4]. The LEO satellites are deployed between 500 and 2000 km to provide extended coverage compared to ground Base Stations (BSs) and low propagation delays compared with higher orbit satellites [3]. LEO satellites are expected to be integrated into 5G and beyond-5G networks to enable network scalability, reinforce the communication service availability and reliability, and upgrade the performance of limited terrestrial networks in un-served/underserved areas [3], [5]. Therefore, LEO satellite is an attractive solution for the main use scenarios in 5G, i.e., Enhanced Mobile Broadband (eMBB), massive Machine Type Communications (mMTC), and Ultra-Reliable and Low-Latency Communications (URLLC) [2], [6].

Due to the high orbital velocities of LEO satellites (up to 7.6 km/s) and small ground coverage in comparison with Geostationary Orbit (GEO) satellites, dense LEO deployments are required to form LEO constellations for providing worldwide and continuous coverage [1], [7]. The frequent topological changes resulting from the high orbital velocities complicate communication between satellites and ground User Terminals (UTs). The large-scale LEO satellites induce intra-system interference due to the side-lobe leakage of antennas. Besides, the coexistence of GEO and LEO causes inter-system interference [4]. Efficient utilization of power budget at satellites and the provision of reliable services necessitate effective interference control.

### A. Previous Works

To manage the interference brought about by dense LEO satellites, multiple antenna technologies and signal processing schemes, such as resource allocation and transmit beamforming, can be employed to keep interference to the unintended user below a predefined level [8], [9]. A coexistence framework of the different satellite networks was presented in [10] and [11]. In particular, [10] analyzed the interference from LEO to GEO network in terms of Bit Error Rate (BER) performance for both uplink and downlink transmissions. The effects of interference factors, the number of LEO satellites, and the angle between LEO and GEO satellites, are investigated. [11] studied the GEO and LEO coexistence system where the LEO satellites serve as primary and the GEO satellite acts as secondary. Beam hopping and adaptive power control techniques are implemented at the GEO satellite to maximize the system throughput and minimize the interference from GEO to the LEO network. Unlike [11], the authors of

[12] and [13] considered a case where the GEO satellite is treated as primary and the LEO as secondary. [12] focused on a single GEO-single LEO co-existing system, and the authors formulated a beam power control problem solved by a fractional programming algorithm aiming to maximize the LEO transmission rate while satisfying the service quality requirement of the GEO satellite. [13] extended the scenario to a single GEO-multiple LEO satellites network, a flexible spectrum sharing and cooperative communication method is proposed to mitigate the inter-system interference, where LEO UTs (LUs) can be served by multiple LEO satellites cooperatively.

In contrast to the works mentioned above that concentrate on power control in non-terrestrial networks, beamforming techniques can also be utilized to coordinate the interference between different satellite systems and improve system performance. Rate Splitting Multiple Access (RSMA), relying on linear precoding rate-splitting at the transmitter and Successive Interference Cancellation (SIC) at the receivers, has emerged as a promising multiple access technique for modern multi-antenna networks. According to [14], RSMA divides user messages into common and private parts at the transmitter. The common parts of the split messages are combined and encoded into a common stream, then decoded by multiple users, while the private parts are encoded separately and decoded by their corresponding users (and treated as noise by co-scheduled users). By exploiting the splitting of user messages, RSMA can softly bridge and thus reconcile the two extreme interference management strategies of treating interference as noise and fully decoding interference [15]–[17]. There are various structures of RSMA, including 1-layer RSMA, multilayer (hierarchical) RSMA, and generalized RSMA. In particular, 1-layer RSMA is practical to implement since the common stream has to be decoded by all users and it only needs one-layer of SIC at each user. The gains of RSMA have been demonstrated in various multi-antenna terrestrial networks in terms of energy efficiency [18], [19], user fairness [20]–[22], robustness and latency [23]–[26] for a wide range of network loads and user channel conditions.

More recently, researchers extended the application of RSMA to satellite communication and Satellite-Terrestrial Integrated Network (STIN). [27] implemented RSMA in a two-beam GEO satellite communication system to mitigate the inter-beam interference and improve the achievable rate region. [28] considered an RSMA-based multibeam multicast network with different Channel State Information at Transmitter (CSIT) qualities, and a Weighted Minimum-Mean Square Error (WMMSE)-based algorithm was proposed to maximize the Max-Min Fairness

(MMF) ergodic rate subject to the power constraint at the satellite. A general STIN framework was presented in [29], in which the satellite users receive the multibeam interference, and cellular users suffer from the inter-cell interference and interference from the satellite. The authors designed two RSMA-based STIN schemes to suppress interference aiming to maximize the minimum fairness rate among all satellite users and cellular users. Simulation results showed that the proposed scheme achieves higher MMF rate than the conventional schemes without RSMA, illustrating the effectiveness of RSMA to manage the interference among satellites. [30] further involved an Unmanned Aerial Vehicle (UAV) into the satellite network, where the GEO satellite adopted multicast transmission and the UAV employed RSMA-based multigroup multicast transmission. Both systems interfere with each other, RSMA is used at the UAV sub-network to mitigate the intra-system interference and improve the system throughput.

### *B. Contributions*

Motivated by the appealing interference management capability of RSMA, we further investigate the application of RSMA in a multilayer satellite network consisting of a GEO satellite sub-network and multiple LEO satellites sub-network to manage the interference in and between both sub-networks. The contributions of this article are summarized as follows:

- 1) We first present a general framework of multilayer network where RSMA is distributedly implemented at both GEO and LEO satellite sub-networks. Both satellite systems share the same radio spectrum resources. The gateway (GW) is deployed to implement centralized control for gathering and managing various kinds of information, and control the whole system through resource allocation and interference management. This framework differs from the prior RSMA STIN papers due to the involvement of LEO satellites and the distributed implementation of RSMA, i.e., Distributed-RSMA (D-RSMA), at both GEO and LEO networks.
- 2) Based on the proposed multilayer D-RSMA framework, we formulate an MMF problem in order to jointly optimize the precoders of GEO and LEO satellites as well as the message splits of RSMA. Instead of focusing on the performance of one of the sub-networks, and maintaining the quality of service for the other sub-network, like [11]–[13], the objective of this paper is to maximize the minimum rate among all GEO UTs (GUs) and LUs subject to power constraints at satellites. To the best of our knowledge, this is the first work in the literature on joint GEO-LEO beamforming design to enhance max-min fairness.

- 3) Due to the nonconvex and mathematical intractable essence of the formulated optimization problem, we transform the original problem into a solvable one by using Semi-Definite Programming (SDP) and first-order Taylor approximation, and then a penalty function-based iterative algorithm is proposed to tackle the optimization problem. Numerical results demonstrate that the proposed D-RSMA scheme can well manage the interference and improve user fairness.

The rest of this paper is organized as follows. The system model, channel models and multilayer D-RSMA scheme are introduced in Section II. The MMF optimization problem is formulated in Section III. The proposed SDP-based iterative optimization algorithm is specified in Section IV. Simulation results illustrating the effectiveness of our proposed scheme are discussed in Section V, followed by the conclusions in Section VI. The major variables adopted in the paper are listed in Table I for ease of reference.

In the remaining sections of this work, matrices, column vectors, and scalars are denoted by boldface uppercase, boldface lowercase, and standard letters, respectively. The operator  $(\cdot)^T$  denotes transpose and  $(\cdot)^H$  denotes conjugate-transpose.  $\lambda_{\max}(\cdot)$  denotes the maximum eigenvalue of the matrix.  $\mathcal{CN}(\zeta, \varphi^2)$  represents a complex Gaussian distribution with mean  $\zeta$  and variance  $\varphi^2$ .  $\text{tr}(\cdot)$  is the trace.  $|\cdot|$  is the absolute value and  $\|\cdot\|$  is the Euclidean norm.  $\mathbb{C}$  denotes the complex space.  $|\mathcal{A}|$  is the cardinality of the set  $\mathcal{A}$ .

## II. SYSTEM MODEL

We consider a multilayer satellite system with a single GEO satellite and  $M$  LEO satellites serving  $N$  single-antenna GUs and  $K$  single-antenna LUs, respectively. GUs are the UTs served by the GEO, and LUs are the UTs served by the LEO satellites. We denote the set of LEO satellites as  $\mathcal{M} = \{1, \dots, M\}$ .  $\mathcal{N} = \{1, \dots, N\}$  and  $\mathcal{K} = \{1, \dots, K\}$  are the sets of UTs served by GEO and LEO, respectively. LUs are divided into  $M$  groups, and  $\mathcal{K}_m$  denotes the set of UTs under the coverage of  $m$ -th LEO satellite.  $\bigcup_{m \in \mathcal{M}} \mathcal{K}_m = \mathcal{K}$ ,  $\mathcal{K}_i \cap \mathcal{K}_j = \emptyset$ ,  $i, j \in \mathcal{M}$ ,  $i \neq j$ . The size of the  $m$ -th group is  $K_m = |\mathcal{K}_m|$ ,  $\forall k \in \mathcal{K}_m$ . GEO and LEO satellites are equipped with  $N_{tg}$  and  $N_{tl}$  feeds array fed reflector antennas, respectively. We assume that the GEO and LEO satellites operate in the same radio spectrum. The satellites are managed by the GW, which acts as a control hub to gather and handle various types of data, apply centralized processing, and oversee the overall system through resource allocation and interference management. We assume that multilayer satellite networks have perfect Channel State Information at Receiver (CSIR) and

TABLE I  
VARIABLE LIST

| Notation               | Definition                               |
|------------------------|--|
| $M$                    | number of LEO satellites                 |
| $N$                    | number of GUs                            |
| $K$                    | number of LUs                            |
| $N_{tg}$               | number of antennas for GEO               |
| $N_{tl}$               | number of antennas for LEO               |
| $\mathbf{h}_{g,n}$     | channels between GEO and GU- $n$         |
| $\mathbf{h}_{g2l,k_m}$ | channels between GEO and LU- $k_m$       |
| $\mathbf{h}_{l,mk_m}$  | channels between LEO- $m$ and LU- $k_m$  |
| $\mathbf{h}_{l2g,mn}$  | channels between LEO- $m$ and GU- $n$    |
| $s_{g,c}$              | common stream from GEO                   |
| $s_{g,d}$              | GUs-designated stream from GEO           |
| $s_{l,m}^{sub}$        | sub-common stream from LEO- $m$          |
| $s_{p,k_m}$            | private stream from LEO- $m$             |
| $\mathbf{w}_c$         | precoders for GEO common                 |
| $\mathbf{w}_d$         | precoders for GEO GUs-designated stream  |
| $\mathbf{p}_{c,m}$     | precoders for LEO- $m$ sub-common stream |
| $\mathbf{p}_{p,k_m}$   | precoders for LEO- $m$ private stream    |

perfect CSIT. Fig. 1 shows a toy example of the system model with 1 GEO and 4 LEO satellites serving  $N = 6$  GUs, and  $K = 8$  LUs. Each LEO satellite serves two LUs.

Due to the spectrum sharing and co-existence GEO/LEO satellites, each user experiences hierarchical multi-user interference. GUs receive inter-system interference from LEO satellites, besides, LUs suffer from inter-LEO interference from unintended LEO satellites as well as from inter-system interference from GEO. The GEO and LEO satellites can exploit various multiple access techniques to manage the interference, such as RSMA, Space Division Multiple Access (SDMA), multicast [31] etc. Inspired by the state-of-the-art RSMA frameworks and the interference coordination capability of RSMA [17], we propose a scheme where RSMA is

distributedly implemented at different satellites, which is denoted as D-RSMA. Different from prior literature which typically deploys traditional RSMA in one network, in this work, the proposed D-RSMA implements RSMA across the networks (i.e., GEO and LEO sub-networks), enabling data sharing and enhancing the ability of interference management. We elaborate on the system model of D-RSMA in this section.

#### A. Signal Transmission Model

We assume that all GUs are interested in the same content, and the multicast message  $G$  is split into a common part,  $G_c$ , and a GUs-designated part,  $G_d$ , in D-RSMA scheme. The unicast messages  $L_1, \dots, L_{K_m}$  for LUs served by the  $m$ -th LEO are split into three parts, namely, a super-common part, a sub-common part and a private part, i.e.,  $L_{k_m} \rightarrow \{L_{c,k_m}^{sup}, L_{c,k_m}^{sub}, L_{p,k_m}\}$ ,  $\forall k_m \in \mathcal{K}_m, m \in \mathcal{M}$ . The superscript “*sup*” and “*sub*” are used to represent the super-common and sub-common parts for LUs messages/streams, respectively. The common message for GUs,  $G_c$ , and all super-common messages for LUs,  $\{\bigcup_{k_m \in \mathcal{K}} L_{c,k}^{sup}\}$ , are combined as  $T_{g,c}$  and encoded

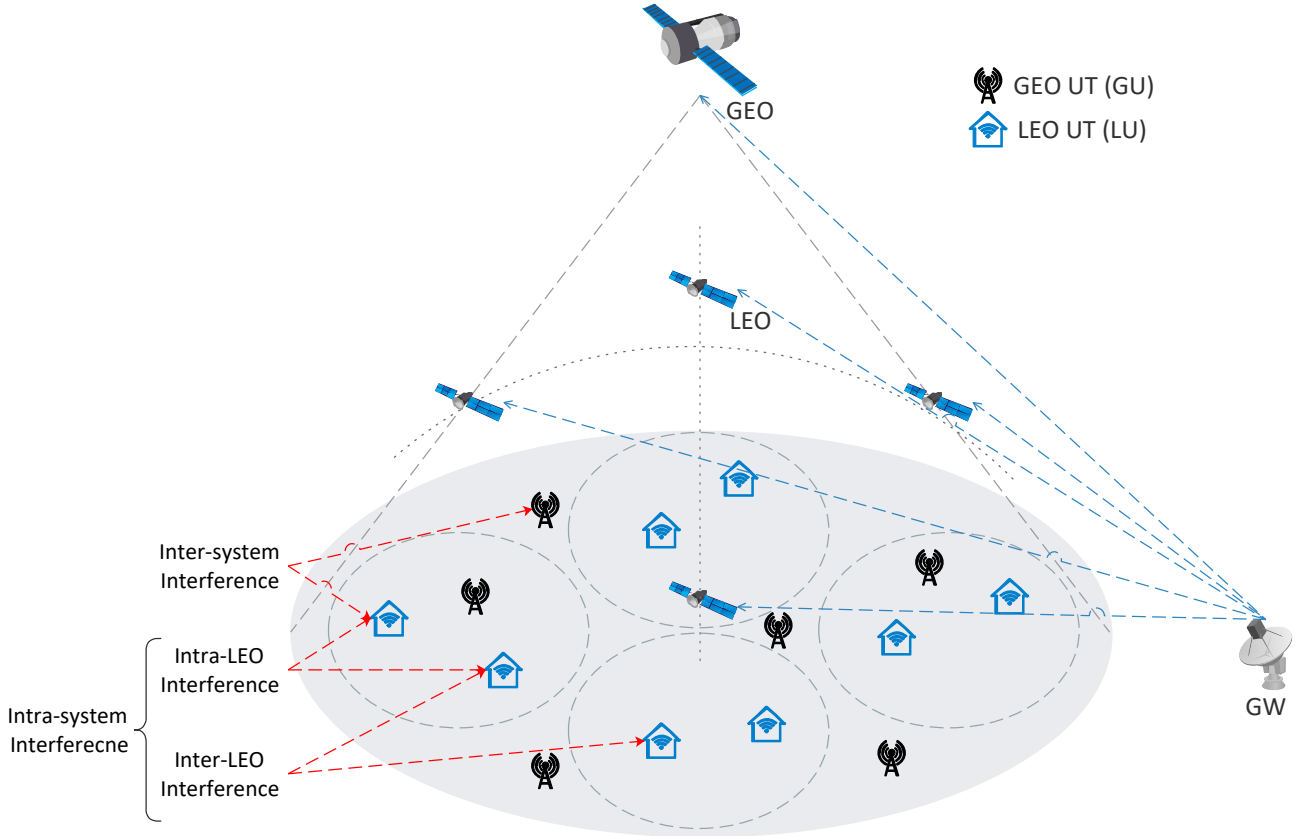


Fig. 1. Multilayered satellite system model with 1 GEO satellite and 4 LEO satellites,  $N = 6$ ,  $K = 8$ .

into  $s_{g,c}$  to be transmitted from GEO and decoded by all GUs and LUs. It manages the inter-system interference between GEO and LEO so as the inter-LEO interference. The GUs-designated message is encoded into  $s_{g,d}$ . The vector of GEO streams  $\mathbf{s}_g = [s_{g,c}, s_{g,d}]^T$  is therefore created, and it obeys  $\mathbb{E} \{\mathbf{s}_g \mathbf{s}_g^H\} = \mathbf{I}$ . The sub-common messages,  $\{\bigcup_{k_m \in \mathcal{K}_m} L_{c,k_m}^{sub}\}$ , for LUs under  $m$ -th LEO coverage are combined into a sub-common message  $T_{l,m}^{sub}$  and encoded into a sub-common stream  $s_{l,m}^{sub}$  to manage the intra-LEO interference. The private parts for LUs are independently encoded into private streams  $s_{p,1}, \dots, s_{p,K_m}$ . The vector of  $m$ -th LEO satellite streams  $\mathbf{s}_{l,m} = [s_{l,m}^{sub}, s_{p,1}, \dots, s_{p,K_m}]^T \in \mathbb{C}^{(K_m+1) \times 1}$  is obtained, and we assume it satisfies  $\mathbb{E} \{\mathbf{s}_{l,m} \mathbf{s}_{l,m}^H\} = \mathbf{I}$ .

Data streams are mapped to the transmit antennas via precoding matrix  $\mathbf{W} = [\mathbf{w}_c, \mathbf{w}_d] \in \mathbb{C}^{N_{tg} \times 2}$  at GEO satellite and precoding matrices  $\mathbf{P}_m = [\mathbf{p}_{c,m}, \mathbf{p}_{p,1}, \dots, \mathbf{p}_{p,K_m}]$  at  $m$ -th LEO satellite, where  $\mathbf{P}_m \in \mathbb{C}^{N_{tl} \times (K_m+1)}$ . The respective transmit signals at the GEO and  $m$ -th LEO are

$$\mathbf{x}_g = \mathbf{w}_c s_{g,c} + \mathbf{w}_d s_{g,d}, \quad (1a)$$

$$\mathbf{x}_{l,m} = \mathbf{p}_{c,m} s_{l,m}^{sub} + \sum_{k_m=1}^{K_m} \mathbf{p}_{p,k_m} s_{p,k_m}, \quad m \in \mathcal{M}. \quad (1b)$$

Following [32], [33], we assume that they are subject to the total power constraints, i.e.,  $\mathbb{E} \{\mathbf{x}_g^H \mathbf{x}_g\} \leq P_g$ , and  $\mathbb{E} \{\mathbf{x}_{l,m}^H \mathbf{x}_{l,m}\} \leq P_l$ . The processes of the received signal at GUs and LUs are illustrated in the following two subsections, respectively.

1) *GEO UT*: After each GEO UT (GU) receives the signal, it first decodes the GEO common stream,  $s_{g,c}$ , by treating other streams as noise. The interference between GEO and LEO satellites and inter-LEO interference are handled by  $s_{g,c}$ , because it contains a portion of UT messages from both GUs and LUs. Each GU or LEO UT (LU) partially decodes the inter-system interference and partially treats inter-system interference as noise, so as to inter-LEO interference for LUs. The signal received at GU- $n$  can be expressed as

$$\begin{aligned} y_{g,n} &= \mathbf{h}_{g,n}^H \mathbf{x}_g + \sum_{m=1}^M \mathbf{h}_{l2g,mn}^H \mathbf{x}_{l,m} + n_n \\ &= \underbrace{\mathbf{h}_{g,n}^H \mathbf{w}_c s_{g,c} + \mathbf{h}_{g,n}^H \mathbf{w}_d s_{g,d}}_{\text{Desired signal}} + \underbrace{\sum_{m=1}^M \mathbf{h}_{l2g,mn}^H (\mathbf{p}_{c,m} s_{l,m}^{sub} + \sum_{i=1}^{K_m} \mathbf{p}_{p,i} s_{p,i})}_{\text{Interference from LEO satellites}} + n_n, \end{aligned} \quad (2)$$

where  $\mathbf{h}_{g,n} \in \mathbb{C}^{N_{tg} \times 1}$  is the channel between the GEO satellite and GU- $n$  and  $\mathbf{h}_{l2g,mn} \in \mathbb{C}^{N_{tl} \times 1}$  is the channel between the  $m$ -th LEO satellite and GU- $n$ ,  $m \in \mathcal{M}$ .  $n_n \sim \mathcal{CN}(0, \sigma_n^2)$  represents



the Additive White Gaussian Noise (AWGN) at GU- $n$ ,  $n \in \mathcal{N}$ . The Signal to Interference plus Noise Ratio (SINR) of decoding the common stream at GU- $n$  is

$$\rho_{g,cn} = \frac{S_{g,cn}}{S_{g,dn} + I_{g,n}^{tot} + \sigma_n^2}, \quad n \in \mathcal{N}, \quad (3)$$

where  $S_{g,cn} = |\mathbf{h}_{g,n}^H \mathbf{w}_c|^2$ ,  $S_{g,dn} = |\mathbf{h}_{g,n}^H \mathbf{w}_d|^2$ .  $I_{g,n}^{tot} = \sum_{m=1}^M |\mathbf{h}_{l2g,mn}^H \mathbf{p}_{c,m}|^2 + \sum_{m=1}^M \sum_{i=1}^{K_m} |\mathbf{h}_{l2g,mn}^H \mathbf{p}_{p,i}|^2$  is the sum of interference power of sub-common streams and the private streams for LUs. The corresponding achievable rate expresses as  $R_{g,cn} = \log_2(1 + \rho_{g,cn})$ . Once  $s_{g,c}$  is decoded, it is subtracted from the received signal. Subsequently, GU- $n$  decodes the GUs-designated stream  $s_{g,d}$ . Accordingly, GU- $n$ 's decoding SINR of the GUs-designated stream writes as

$$\rho_{g,dn} = \frac{S_{g,dn}}{I_{g,n}^{tot} + \sigma_n^2}, \quad n \in \mathcal{N}. \quad (4)$$

The designated rate of GU- $n$  is expressed as  $R_{g,dn} = \log_2(1 + \rho_{g,dn})$ . GU- $n$  reconstructs the original message after the common and GUs-designated messages have been decoded by taking the decoded  $G_c$  from the decoded  $T_{g,c}$  and combining it with the decoded  $G_d$ .

2) *LEO UT*: The received signal at LU- $k_m$  writes as

$$\begin{aligned} y_{l,k_m} &= \mathbf{h}_{l,mk_m}^H \mathbf{x}_{l,m} + \mathbf{h}_{g2l,k_m}^H \mathbf{x}_g + \sum_{\substack{j=1, \\ j \neq m}}^M \mathbf{h}_{l,jk_m}^H \mathbf{x}_{l,j} + n_{k_m} \\ &= \underbrace{\mathbf{h}_{g2l,k_m}^H \mathbf{w}_c s_{g,c} + \mathbf{h}_{l,mk_m}^H \mathbf{p}_{c,m} s_{l,m}^{sub} + \mathbf{h}_{l,mk_m}^H \mathbf{p}_{p,k_m} s_{p,k_m}}_{\text{Desired signal}} + \underbrace{\mathbf{h}_{l,mk_m}^H \sum_{\substack{i=1, \\ i \neq k_m}}^{K_m} \mathbf{p}_{p,i} s_{p,i}}_{\text{Intra-LEO interference}} \\ &\quad + \underbrace{\mathbf{h}_{g2l,k_m}^H \mathbf{w}_d s_{g,d}}_{\text{Interference from GEO satellite}} + \underbrace{\sum_{\substack{j=1, \\ j \neq m}}^M \mathbf{h}_{l,jk_m}^H \left( \mathbf{p}_{c,j} s_{l,j}^{sub} + \sum_{i=1}^{K_j} \mathbf{p}_{p,i} s_{p,i} \right)}_{\text{Inter-LEO interference}} + n_{k_m}, \end{aligned} \quad (5)$$

where  $\mathbf{h}_{l,mk_m} \in \mathbb{C}^{N_{ul} \times 1}$  is the channel between the  $m$ -th LEO satellite and LU- $k_m$  and  $\mathbf{h}_{g2l,k_m} \in \mathbb{C}^{N_{ig} \times 1}$  is the channel between the GEO satellite and LU- $k_m$ .  $n_{k_m} \sim \mathcal{CN}(0, \sigma_{k_m}^2)$  represents the AWGN at LU- $k_m$ ,  $k_m \in \mathcal{K}_m$ ,  $m \in \mathcal{M}$ . The SINR of decoding the  $s_{g,c}$  at LU- $k_m$  is given by

$$\rho_{l,k_m}^{sup} = \frac{S_{g2l,ck_m}}{S_{l,ck_m} + S_{l,pk_m} + I_{l,k_m}^{tot} + \sigma_{k_m}^2}, \quad k_m \in \mathcal{K}_m, \quad (6)$$

where  $S_{g2l,ck_m} = |\mathbf{h}_{g2l,k_m}^H \mathbf{w}_c|^2$ ,  $S_{l,ck_m} = |\mathbf{h}_{l,mk_m}^H \mathbf{p}_{c,m}|^2$ ,  $S_{l,pk_m} = |\mathbf{h}_{l,mk_m}^H \mathbf{p}_{p,k_m}|^2$ .  $I_{l,k_m}^{tot} = \sum_{\substack{i=1, \\ i \neq k_m}}^{K_m} |\mathbf{h}_{l,mk_m}^H \mathbf{p}_{p,i}|^2 + \sum_{\substack{j=1, \\ j \neq m}}^M |\mathbf{h}_{l,jk_m}^H \mathbf{p}_{c,j}|^2 + \sum_{\substack{j=1, \\ j \neq m}}^M \sum_{i=1}^{K_j} |\mathbf{h}_{l,jk_m}^H \mathbf{p}_{p,i}|^2 + |\mathbf{h}_{g2l,k_m}^H \mathbf{w}_d|^2$  is the sum of interference power

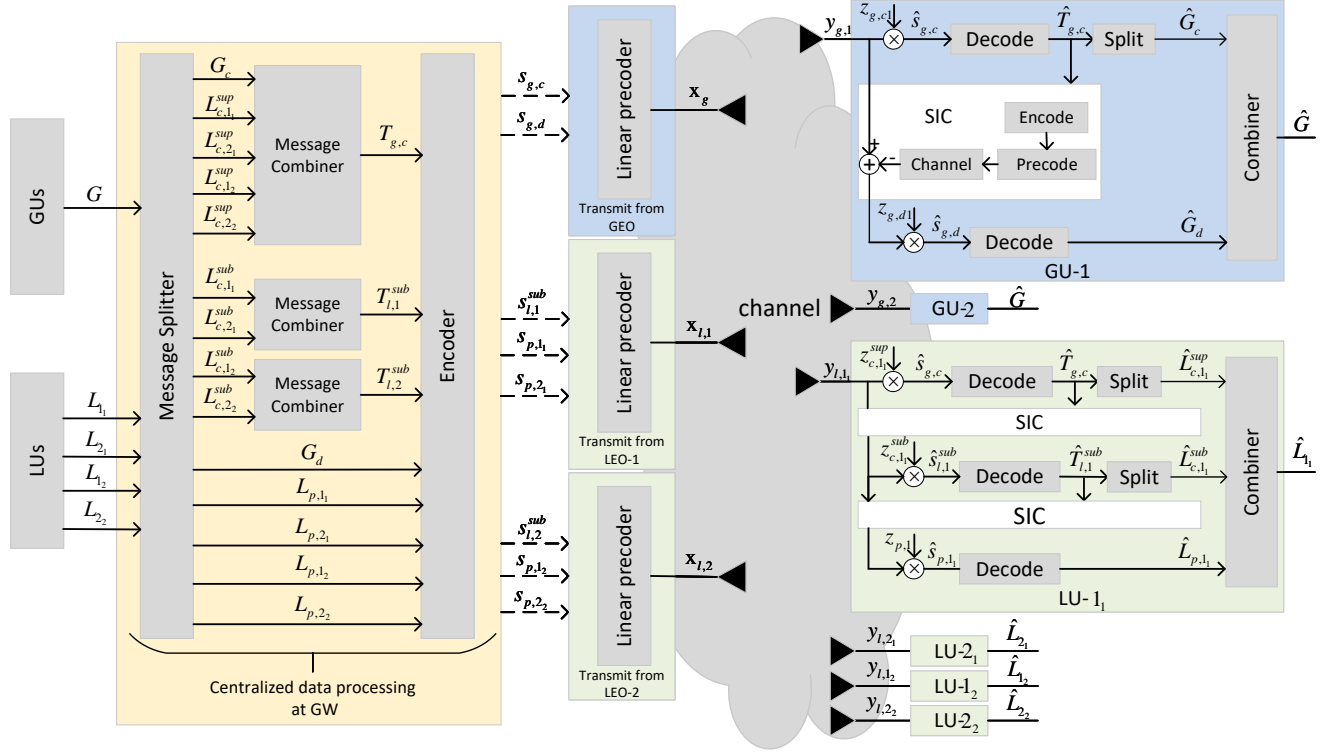


Fig. 2. D-RSMA signal transmission model for 1 GEO and 2 LEO satellites deployment,  $N = 2$ ,  $M = 4$ , each LEO satellite serves 2 LUs.

received at LU- $k_m$ . The corresponding rate is  $R_{l,k_m}^{sup} = \log_2(1 + \rho_{l,k_m}^{sup})$ . In order to make sure that all GUs and LUs can decode  $s_{g,c}$ , we define the common rate

$$R_c = \min_{n \in \mathcal{N}, k \in \mathcal{K}} \{R_{g,cn}, R_{l,k}^{sup}\}. \quad (7)$$

Since  $s_{g,c}$  is shared among all GUs and LUs, we define  $R_c \triangleq \sum_{n=1}^N C_{g,n} + \sum_{m=1}^M \sum_{k_m=1}^{K_m} C_{l,k_m}^{sup}$ , where  $C_{g,n}$  and  $C_{l,k_m}^{sup}$  denote the  $n$ -th GU's and  $k_m$ -th LU's portions of common rate, respectively.

Once  $s_{g,c}$  is decoded, its contribution to the original received signal  $y_{l,k_m}$  is subtracted through SIC. After that, LU- $k_m$  decodes its sub-common stream  $s_{l,m}^{sub}$  by treating other sub-common streams as noise. The sub-common streams are used to manage intra-LEO interference since it contains parts of messages for LUs served by the same LEO. Sub-common streams enable users to partially decode intra-LEO interference and partially treat intra-LEO interference as noise. The SINR of decoding the sub-common stream  $s_{l,m}^{sub}$  at LU- $k_m$  served by LEO- $m$  is

$$\rho_{l,k_m}^{sub} = \frac{S_{l,ck_m}}{S_{l,pk_m} + I_{l,k_m}^{tot} + \sigma_{k_m}^2}, \quad k_m \in \mathcal{K}_m. \quad (8)$$

The rate of the sub-common stream is  $R_{l,k_m}^{sub} = \log_2(1 + \rho_{l,k_m}^{sub})$ . To guarantee that all LUs served by  $m$ -th LEO are capable of decoding  $s_{l,m}^{sub}$ , we define the achievable sub-common rates as

$$R_{c,m}^{sub} = \min_{k_m \in \mathcal{K}_m} \{R_{l,k_m}^{sub}\} = \sum_{k_m=1}^{K_m} C_{l,k_m}^{sub}, \quad (9)$$

where  $C_{l,k_m}^{sub}$  is the rate at which  $L_{c,k_m}^{sub}$  is communicated. After the sub-common stream is decoded, re-encoded, precoded, and subtracted from the received signal through SIC, LU- $k_m$  decodes its private stream  $s_{k_m}$ . The SINR of decoding the private stream  $s_{k_m}$  at LU- $k_m$  is

$$\rho_{k_m} = \frac{S_{l,pk_m}}{I_{l,k_m}^{tot} + \sigma_{k_m}^2}, \quad k_m \in \mathcal{K}_m. \quad (10)$$

The corresponding private rate is  $R_{p,k_m} = \log_2(1 + \rho_{k_m})$ . Thus, the achievable rates of GU- $n$  and LU- $k_m$  are respectively given as

$$R_n = C_{g,n} + R_{g,dn}, \quad n \in \mathcal{N}, \quad (11a)$$

$$R_{k_m} = C_{l,k_m}^{sup} + C_{l,k_m}^{sub} + R_{p,k_m}, \quad k_m \in \mathcal{K}_m, \quad m \in \mathcal{M}. \quad (11b)$$

A signal transmission model for D-RSMA is shown in Fig. 2.

*Remark 1:* D-RSMA is designed for managing interference of the co-existence GEO/LEO satellites multilayer network. Each GU decodes  $s_{g,c}$  first and requires 1 layer of SIC to decode  $s_{g,d}$ . By decoding  $s_{g,c}$ , the inter-system interference can be suppressed since partial inter-system interference is decoded and part of inter-system interference is treated as noise. While each LU requires 2 layers of SIC before decoding intended private stream (in order to decode  $s_{g,c}$  first and then decode  $s_{l,m}^{sub}$ ). The inter-system interference and inter-LEO interference is managed through  $s_{g,c}$ , and the intra-LEO interference is managed by  $s_{l,m}^{sub}$ .

D-RSMA is a general framework of multilayer network that encompasses traditional RSMA and SDMA as special cases. By switching off  $s_{g,c}$ , the multiple access technique of GEO sub-network becomes traditional multicasting, and the multiple access approach of LEO sub-network reduces to 1-layer RSMA. By turning off  $s_{g,c}$  and sub-common streams, GEO and LEO sub-networks work in multicasting and SDMA manner, respectively.

## B. Channel Model

In this subsection, we illustrate the channel models of GEO and LEO satellites.

1) *GEO Satellite Channel*: We assume that the channel realizations between the satellite and different UTs are uncorrelated, because different UTs are often geographically separated by a certain distance. The main characteristics of GEO channel include atmospheric fading and radiation pattern. Rain attenuation is the dominant atmospheric impact for the Ka-band satellite channel, and it is often characterized by a lognormal distribution [28], [29]. The GEO satellite channel vector between the satellite and  $i$ -th UT is expressed as  $\mathbf{h}_{g,i} = [h_{g,1i}, h_{g,2i}, \dots, h_{g,N_{tg}i}]^T$ ,  $i \in \mathcal{N} \cup \mathcal{K}$ . The  $n_{tg}$ -th entry of the channel between the GEO satellite and the UT- $i$  can be written as

$$h_{g,n_{tg}i} = \frac{\sqrt{G_r G_{g,i}}}{4\pi \frac{d_{g,i}}{\lambda} \sqrt{\kappa T_{sys} B_w}} \chi_{n_{tg}i}^{-\frac{1}{2}} e^{-j\phi_{g,n_{tg}i}}, i \in \{\mathcal{N} \cup \mathcal{K}\}, \quad (12)$$

where  $G_r$  and  $G_{g,i}$  are the UT antenna gain and the antenna gain from GEO satellite to the UT- $i$ , respectively.  $d_{g,i}$  and  $\lambda$  denote the distance from the GEO satellite to UT- $i$  and the carrier wavelength, respectively.  $\kappa$  is the Boltzmann constant,  $T_{sys}$  is the receiving system noise temperature and  $B_w$  denotes the user link bandwidth. The large-scale fading is modeled as  $\chi_{n_{tg}i,dB} = 10 \log_{10}(\chi_{n_{tg}i})$ , and  $\ln(\chi_{n_{tg}i,dB}) \sim \mathcal{N}(\mu, \sigma)$ .  $\phi_{g,i} = [\phi_{g,1i}, \phi_{g,2i}, \dots, \phi_{N_{tg}i}]^T \in \mathbb{R}^{N_{tg} \times 1}$  is channel phase vector.  $G_{g,i}$  can be further expressed as

$$G_{g,i} = G_{max} \left[ \frac{J_1(u_{g,i})}{2u_{g,i}} + 36 \frac{J_3(u_{g,i})}{u_{g,i}^3} \right]^2, \quad (13)$$

where  $u_{g,i} = 2.07123 \frac{\sin(\theta_{g,i})}{\sin(\theta_{3dB})}$ .  $\theta_{g,i}$  is the angle between UT- $i$  and the center of GEO satellite beam.  $\theta_{3dB}$  denotes a 3 dB loss angle compared with the beam center.  $G_{max}$  is the maximum beam gain of the beam center.  $J_1$  and  $J_3$  are first-kind Bessel functions with first-order and third-order, respectively. The channel between GEO and LU- $k_m$  is  $\mathbf{h}_{g2l,k_m} = [h_{g,1k_m}, h_{g,2k_m}, \dots, h_{g,N_{tg}k_m}]^T$ ,  $k_m \in \mathcal{K}_m, m \in \mathcal{M}$ .

2) *LEO Satellite Channel*: Due to the high mobility of LEO, the propagation characteristics of satellite channel and impact on the channel modelling are different. It differs from GEO satellite channel due to the Doppler shift and delay [33], [34]. The Doppler shift  $f_{i,u}$  associated with propagation path  $u$  of UT- $i$  is dominated by two independent Doppler shifts,  $f_{i,u}^{sat}$  and  $f_{i,u}^{ut}$ , which result from the movements of LEO satellite and UT, respectively. The channel between  $m$ -th LEO satellite and  $i$ -th UT is

$$\mathbf{h}_{l,mi} = g_{mi}(t, f) e^{j2\pi(f_{i,u}^{sat} t - f\tau_i^{\min})} e^{-j\phi_{l,mi}}, \quad (14a)$$

$$g_{mi}(t, f) = \sum_{u=0}^{U_i-1} g_{i,u} e^{j2\pi(f_{i,u}^{ut} t - f\tau_{i,u}^{ut})}, i \in \{\mathcal{N} \cup \mathcal{K}\}, \quad (14b)$$

where  $\tau_i^{\min}$  is the minimum value of the propagation delays of the  $i$ -th UT defined by  $\tau_i^{\min} = \min_u \{\tau_{i,u}\}$ , where  $\tau_{i,u}$  is the delay of the  $u$ -th path to UT- $i$ . We denote the delay difference of UT- $i$  with path  $u$  as  $\tau_{i,u}^{ut} \triangleq \tau_{i,u} - \tau_i^{\min}$ .  $U_i$  denotes the number of propagation paths of the  $i$ -th UT. The Doppler shift  $f_{i,u}^{sat}$  induced by the movement of the LEO satellite can be considered to be identical for different propagation paths of the same UT- $i$  due to the relatively high altitude of the LEO satellite [34], [35]. Hence, in order to simplify the notation, we recast and omit the path index the Doppler shifts caused by the motion of the LEO satellite as  $f_{i,u}^{sat} = f_i^{sat}$ .  $\phi_{l,mi}$  is the channel angle vector from LEO satellite- $m$  to UT- $i$ .  $\phi_{l,mi} = [\phi_{1i}^{l,m}, \phi_{2i}^{l,m}, \dots, \phi_{N_{li}}^{l,m}]^T \in \mathbb{R}^{N_{li} \times 1}$  is channel phase vector, and it can be calculated by using geographic location information between the  $i$ -th UT and the LEO satellite, or it can be acquired through using satellite positioning system [36].  $g_{mi}(t, f)$  is LEO satellite downlink channel gain,  $g_{i,u}$  is the complex-valued gain corresponding to path  $u$  and UT- $i$  [37]. LEO satellite system usually operates under Line-of-Sight (LoS) propagations, and we assume  $g_{mi}(t, f)$  follows Rician fading distribution with the Rician factor  $\kappa_i$  and power

$$\gamma_i = \mathbb{E} \{|g_i(t, f)|^2\} = \frac{G_r G_l}{(4\pi \frac{d_{mi}}{\lambda})^2 \kappa T_{sys} B_w}, \quad (15)$$

where  $G_l$  is the antenna gain of the LEO satellite. Alternatively, the real and imaginary parts of  $g_{mi}(t, f)$  have independent and identically distributed (i.i.d) real-valued Gaussian entries with a certain mean and variance, i.e.,  $g_{mi}(t, f) \sim \mathcal{N}\left(\sqrt{\frac{\kappa_i \gamma_i}{2(\kappa_i + 1)}}, \frac{\gamma_i}{2(\kappa_i + 1)}\right)$ .

We assume that the time and frequency synchronizations can be performed perfectly. Specifically, the Doppler compensation,  $f_i^{syn} = f_i^{sat}$ , and delay compensation,  $\tau_i^{syn} = \tau_i^{\min}$  are applied [34], [38]. The LEO channel for the  $k$ -th LU can be equivalently expressed as  $\mathbf{h}_{l,mk}^{syn} = g_{mk}(t, f)e^{-j\phi_{l,mk}}$ ,  $k \in \mathcal{K}$ ,  $m \in \mathcal{M}$ . The interference channel between LEO- $m$  satellites and GU- $n$  writes as  $\mathbf{h}_{l2g,mn} = \mathbf{h}_{l,mn}$ ,  $n \in \mathcal{N}$ ,  $m \in \mathcal{M}$ , with corresponding synchronized channel  $\mathbf{h}_{l2g,mn}^{syn} = g_{mn}(t, f)e^{-j\phi_{l,mn}}$ .

### III. PROBLEM FORMULATION

In this section, we focus on designing a joint optimization of GEO-LEO beamforming problem that maximizes the minimum fairness rate across all GUs and LUs under the constraint of transmit

power at all satellites. For D-RSMA based multilayer satellite network, the optimization problem can be formulated as

$$\mathcal{P}_1 : \max_{\mathbf{c}, \mathbf{W}, \mathbf{P}} \min_{n \in \mathcal{N}, k \in \mathcal{K}} \{R_n, R_k\} \quad (16a)$$

$$\text{s.t.} \quad \sum_{n \in \mathcal{N}} C_{g,n} + \sum_{k \in \mathcal{K}} C_{l,k_m}^{sup} \leq R_c \quad (16b)$$

$$\sum_{k_m \in \mathcal{K}_m} C_{l,k_m}^{sub} \leq R_{c,m}^{sub}, \quad m \in \mathcal{M} \quad (16c)$$

$$\text{tr}(\mathbf{W}\mathbf{W}^H) \leq P_g \quad (16d)$$

$$\text{tr}(\mathbf{P}_m \mathbf{P}_m^H) \leq P_l, \quad m \in \mathcal{M} \quad (16e)$$

$$\mathbf{c} \succeq \mathbf{0}, \quad (16f)$$

where  $\mathbf{P} = [\mathbf{P}_1, \dots, \mathbf{P}_M]$  represents the precoding matrix at all LEO satellites.  $\mathbf{c} = [\mathbf{c}_g, \mathbf{c}_l^{sup}, \mathbf{c}_l^{sub}]$ , where  $\mathbf{c}_g = [C_{g,1}, \dots, C_{g,N}]^T$ ,  $\mathbf{c}_l^{sup} = [C_{l,1}^{sup}, \dots, C_{l,K}^{sup}]^T$ , and  $\mathbf{c}_l^{sub} = [C_{l,1}^{sub}, \dots, C_{l,K}^{sub}]^T$  are the vectors of common rate portions. (16b) ensures that all GUs and LUs can successfully decode the common stream  $s_{g,c}$ . Similarly, (16c) guarantees that the sub-common stream  $s_{l,m}^{sub}$  can be decoded by all LUs under the coverage of LEO- $m$ . (16d) and (16e) represent power constraints of the GEO and LEO satellites. (16f) ensure that all common rate portions are non-negative.

#### IV. PROPOSED ALGORITHM

The formulated problem (16) is nonconvex, while it can be transformed into a tractable SDP problem and solved with rank-one constraints. An SDP-based iterative optimization algorithm is proposed in this section. Denote  $\alpha = \{\alpha_{g,c}, \alpha_{g,p}, \alpha_l^{sup}, \alpha_l^{sub}, \alpha_p\}$  and  $F = \{\mathbf{F}_{g,c}, \mathbf{F}_{g,d}, \mathbf{F}_{l,cm}, \mathbf{F}_{l,pk} | k \in \mathcal{K}, m \in \mathcal{M}\}$ , where  $\mathbf{F}_{g,c} = \mathbf{w}_c \mathbf{w}_c^H$ ,  $\mathbf{F}_{g,d} = \mathbf{w}_d \mathbf{w}_d^H$ ,  $\{\mathbf{F}_{l,cm} = \mathbf{p}_{c,m} \mathbf{p}_{c,m}^H\}_{m=1}^M$  and  $\{\mathbf{F}_{l,pk} = \mathbf{p}_{l,pk} \mathbf{p}_{l,pk}^H\}_{k=1}^K$ . By introducing auxiliary variables  $t$ ,  $\alpha$  and  $F$ , the equivalent reformu-

lation of  $\mathcal{P}_1$  is

$$\mathcal{P}_2 : \quad \max_{F, \boldsymbol{\alpha}, \mathbf{c}} \quad t \quad (17a)$$

$$\text{s.t.} \quad t \leq C_{g,n} + \alpha_{g,dn}, \quad n \in \mathcal{N} \quad (17b)$$

$$\sum_{n=1}^N C_{g,n} + \sum_{k=1}^K C_{l,k}^{sup} \leq \alpha_{g,cn}, \quad n \in \mathcal{N} \quad (17c)$$

$$t \leq C_{l,k_m}^{sup} + C_{l,k_m}^{sub} + \alpha_{p,k_m}, \quad k_m \in \mathcal{K}_m, m \in \mathcal{M} \quad (17d)$$

$$\sum_{n=1}^N C_{g,n} + \sum_{k=1}^K C_{l,k}^{sup} \leq \alpha_{l,k_m}^{sup}, \quad k_m \in \mathcal{K}_m, m \in \mathcal{M} \quad (17e)$$

$$\sum_{k_m=1}^{K_m} C_{l,k_m}^{sub} \leq \alpha_{l,k_m}^{sub}, \quad k_m \in \mathcal{K}_m, m \in \mathcal{M} \quad (17f)$$

$$\text{tr}(\mathbf{F}_{g,c}) + \text{tr}(\mathbf{F}_{g,d}) \leq P_g \quad (17g)$$

$$\text{tr}(\mathbf{F}_{l,cm}) + \sum_{k_m=1}^{K_m} \text{tr}(\mathbf{F}_{l,pk_m}) \leq P_l, \quad m \in \mathcal{M} \quad (17h)$$

$$\mathbf{F}_{g,c} \succeq 0, \quad \mathbf{F}_{g,d} \succeq 0 \quad (17i)$$

$$\mathbf{F}_{l,cm} \succeq 0, \quad \mathbf{F}_{l,pk_m} \succeq 0, \quad k_m \in \mathcal{K}_m, \quad m \in \mathcal{M} \quad (17j)$$

$$\text{rank}(\mathbf{F}_{g,c}) = 1, \quad \text{rank}(\mathbf{F}_{g,d}) = 1 \quad (17k)$$

$$\text{rank}(\mathbf{F}_{l,cm}) = 1, \quad \text{rank}(\mathbf{F}_{l,pk_m}) = 1, \quad k_m \in \mathcal{K}_m, m \in \mathcal{M} \quad (17l)$$

$$\mathbf{c} \succeq \mathbf{0}, \quad (17m)$$

where  $\boldsymbol{\alpha}_{g,c} \triangleq [\alpha_{g,c1}, \dots, \alpha_{g,cN}]^T$ ,  $\boldsymbol{\alpha}_{g,p} \triangleq [\alpha_{g,p1}, \dots, \alpha_{g,dN}]^T$ ,  $\boldsymbol{\alpha}_l^{sup} \triangleq [\alpha_{l,1}^{sup}, \dots, \alpha_{l,K}^{sup}]^T$ ,  $\boldsymbol{\alpha}_l^{sub} \triangleq [\alpha_{l,1}^{sub}, \dots, \alpha_{l,K}^{sub}]^T$ ,  $\boldsymbol{\alpha}_p \triangleq [\alpha_{p,1}, \dots, \alpha_{p,K}]^T$  represent the lower bound of corresponding achievable rates. (17g) and (17h) are the equivalent transmit power constraints.

Due to the nonconvex nature of problem (17), we denote  $\mathbf{H}_{g,n} = \mathbf{h}_{g,n} \mathbf{h}_{g,n}^H$  as symmetric GEO channel matrix. Similarly,  $\mathbf{H}_{l2g,mn} = \mathbf{h}_{l2g,mn} \mathbf{h}_{l2g,mn}^H$ ,  $\mathbf{H}_{l,mk_m} = \mathbf{h}_{l,mk_m} \mathbf{h}_{l,mk_m}^H$  and  $\mathbf{H}_{g2l,k_m} = \mathbf{h}_{g2l,k_m} \mathbf{h}_{g2l,k_m}^H$ . Based on the symmetric channel matrixes and beamforming matrixes, the power

segments of the received signal can be reformulated as

$$S'_{g,cn} = \text{tr}(\mathbf{H}_{g,n} \mathbf{F}_{g,c}) \quad (18a)$$

$$S'_{g,dn} = \text{tr}(\mathbf{H}_{g,n} \mathbf{F}_{g,d}) \quad (18b)$$

$$I_{g,n}^{tot'} = \sum_{m=1}^M \text{tr}(\mathbf{H}_{l2g,mn} \mathbf{F}_{l,cm}) + \sum_{m=1}^M \sum_{i=1}^{K_m} \text{tr}(\mathbf{H}_{l2g,mn} \mathbf{F}_{l,pi}) \quad (18c)$$

$$S'_{g2l,ck_m} = \text{tr}(\mathbf{H}_{g2l,k_m} \mathbf{F}_{g,c}) \quad (18d)$$

$$S'_{l,ck_m} = \text{tr}(\mathbf{H}_{l,mk_m} \mathbf{F}_{l,cm}) \quad (18e)$$

$$S'_{l,pk_m} = \text{tr}(\mathbf{H}_{l,mk_m} \mathbf{F}_{l,pk_m}) \quad (18f)$$

$$\begin{aligned} I_{l,k_m}^{tot'} &= \sum_{\substack{i=1, \\ i \neq k_m}}^{K_m} \text{tr}(\mathbf{H}_{l,mk_m} \mathbf{F}_{l,pi}) + \sum_{\substack{j=1, \\ j \neq m}}^M \text{tr}(\mathbf{H}_{l,jk_m} \mathbf{F}_{l,cj}) \\ &\quad + \sum_{\substack{j=1, \\ j \neq m}}^M \sum_{i=1}^{K_j} \text{tr}(\mathbf{H}_{l,jk_m} \mathbf{F}_{l,pi}) + \text{tr}(\mathbf{H}_{g2l,k_m} \mathbf{F}_{g,d}). \end{aligned} \quad (18g)$$

Therefore, the rate expressions can be redefined as

$$R'_{g,cn} = \log_2(1 + \frac{S'_{g,cn}}{S'_{g,dn} + I_{g,n}^{tot'} + \sigma_n^2}) \quad (19a)$$

$$R'_{g,dn} = \log_2(1 + \frac{S'_{g,dn}}{I_{g,n}^{tot'} + \sigma_n^2}) \quad (19b)$$

$$R_{l,k_m}^{sup'} = \log_2(1 + \frac{S'_{g2l,ck_m}}{S'_{l,ck_m} + S'_{l,pk_m} + I_{l,k_m}^{tot'} + \sigma_{k_m}^2}) \quad (19c)$$

$$R_{l,k_m}^{sub'} = \log_2(1 + \frac{S'_{l,ck_m}}{S'_{l,pk_m} + I_{l,k_m}^{tot'} + \sigma_{k_m}^2}) \quad (19d)$$

$$R'_{p,k_m} = \log_2(1 + \frac{S'_{l,pk_m}}{I_{l,k_m}^{tot'} + \sigma_{k_m}^2}). \quad (19e)$$

In order to solve the non-convex parts in the rate expressions, we further introduce slack variables  $\boldsymbol{\eta} = \{\boldsymbol{\eta}_{g,c}, \boldsymbol{\eta}_{g,p}, \boldsymbol{\eta}_l^{sup}, \boldsymbol{\eta}_l^{sub}, \boldsymbol{\eta}_p\}$  and  $\boldsymbol{\xi} = \{\boldsymbol{\xi}_{g,c}, \boldsymbol{\xi}_{g,p}, \boldsymbol{\xi}_l^{sup}, \boldsymbol{\xi}_l^{sub}, \boldsymbol{\xi}_p\}$ , where  $\boldsymbol{\eta}_{g,c} \triangleq [\eta_{g,c1}, \dots, \eta_{g,cN}]^T$ ,  $\boldsymbol{\eta}_{g,p} \triangleq [\eta_{g,p1}, \dots, \eta_{g,pN}]^T$ ,  $\boldsymbol{\eta}_l^{sup} \triangleq [\eta_{l,1}^{sup}, \dots, \eta_{l,K}^{sup}]^T$ ,  $\boldsymbol{\eta}_l^{sub} \triangleq [\eta_{l,1}^{sub}, \dots, \eta_{l,K}^{sub}]^T$ ,  $\boldsymbol{\eta}_p \triangleq [\eta_{p,1}, \dots, \eta_{p,K}]^T$ .  $\boldsymbol{\xi}_{g,c} \triangleq [\xi_{g,c1}, \dots, \xi_{g,cN}]^T$ ,  $\boldsymbol{\xi}_{g,p} \triangleq [\xi_{g,p1}, \dots, \xi_{g,pN}]^T$ ,  $\boldsymbol{\xi}_l^{sup} \triangleq [\xi_{l,1}^{sup}, \dots, \xi_{l,K}^{sup}]^T$ ,  $\boldsymbol{\xi}_l^{sub} \triangleq [\xi_{l,1}^{sub}, \dots, \xi_{l,K}^{sub}]^T$ ,  $\boldsymbol{\xi}_p \triangleq [\xi_{p,1}, \dots, \xi_{p,K}]^T$ . By taking GU- $n$ 's lower bound of private rate



as an example,  $\alpha_{g,dn} \leq R'_{g,dn}$ , it can be transformed as

$$\alpha_{g,dn} \ln 2 \leq \ln\left(\frac{S'_{g,dn} + I_{g,n}^{tot'} + \sigma_n^2}{I_{g,n}^{tot'} + \sigma_n^2}\right) \quad (20a)$$

$$= \ln(S'_{g,dn} + I_{g,n}^{tot'} + \sigma_n^2) - \ln(I_{g,n}^{tot'} + \sigma_n^2) \quad (20b)$$

$$= \eta_{g,dn} - \xi_{g,dn}, \quad (20c)$$

where  $\eta_{g,dn}$  and  $\xi_{g,dn}$  represent the lower bound and upper bound of corresponding terms, respectively.

Based on the auxiliary variables,  $\mathcal{P}_2$  can be rewritten as  $\mathcal{P}_3$ .

$$\mathcal{P}_3 : \quad \max_{\substack{F, \alpha, c \\ \eta, \xi}} \quad t \quad (21a)$$

$$\text{s.t.} \quad \alpha_{g,cn} \ln 2 \leq \eta_{g,cn} - \xi_{g,cn}, \quad n \in \mathcal{N} \quad (21b)$$

$$S'_{g,cn} + S'_{g,dn} + I_{g,n}^{tot'} + \sigma_n^2 \geq e^{\eta_{g,cn}} \quad (21c)$$

$$S'_{g,dn} + I_{g,n}^{tot'} + \sigma_n^2 \leq e^{\xi_{g,cn}} \quad (21d)$$

$$\alpha_{g,dn} \ln 2 \leq \eta_{g,dn} - \xi_{g,dn}, \quad n \in \mathcal{N} \quad (21e)$$

$$S'_{g,dn} + I_{g,n}^{tot'} + \sigma_n^2 \geq e^{\eta_{g,dn}} \quad (21f)$$

$$I_{g,n}^{tot'} + \sigma_n^2 \leq e^{\xi_{g,dn}} \quad (21g)$$

$$\alpha_{l,k_m}^{sup} \ln 2 \leq \eta_{l,k_m}^{sup} - \xi_{l,k_m}^{sup}, \quad k_m \in \mathcal{K}_m, \quad m \in \mathcal{M} \quad (21h)$$

$$S'_{g2l,ck_m} + S'_{l,ck_m} + S'_{l,pk_m} + I_{l,k_m}^{tot'} + \sigma_n^2 \geq e^{\eta_{l,k_m}^{sup}} \quad (21i)$$

$$S'_{l,ck_m} + S'_{l,pk_m} + I_{l,k_m}^{tot'} + \sigma_n^2 \leq e^{\xi_{l,k_m}^{sup}} \quad (21j)$$

$$\alpha_{l,k_m}^{sub} \ln 2 \leq \eta_{l,k_m}^{sub} - \xi_{l,k_m}^{sub}, \quad k_m \in \mathcal{K}_m, \quad m \in \mathcal{M} \quad (21k)$$

$$S'_{l,ck_m} + S'_{l,pk_m} + I_{l,k_m}^{tot'} + \sigma_n^2 \geq e^{\eta_{l,k_m}^{sub}} \quad (21l)$$

$$S'_{l,pk_m} + I_{l,k_m}^{tot'} + \sigma_n^2 \leq e^{\xi_{l,k_m}^{sub}} \quad (21m)$$

$$\alpha_{p,k_m} \ln 2 \leq \eta_{p,k_m} - \xi_{p,k_m}, \quad k_m \in \mathcal{K}_m, \quad m \in \mathcal{M} \quad (21n)$$

$$S'_{l,pk_m} + I_{l,k_m}^{tot'} + \sigma_n^2 \geq e^{\eta_{p,k_m}} \quad (21o)$$

$$I_{l,k_m}^{tot'} + \sigma_n^2 \leq e^{\xi_{p,k_m}} \quad (21p)$$

$$(17b) - (17m).$$

Note that (21d), (21g), (21j), (21m) and (21p) are nonconvex with convex Right-Hand Side (RHS) which can be approximated by the first-order Taylor series. The RHS parts of the above constraints are approximated at  $\left\{ \xi_{g,cn}^{[i]}, \xi_{g,dn}^{[i]}, \xi_{l,k_m}^{sup [i]}, \xi_{l,k_m}^{sub [i]}, \xi_{p,k_m}^{[i]} | n \in \mathcal{N}, k_m \in \mathcal{K}_m, m \in \mathcal{M} \right\}$  at iteration  $i$  as (22)

$$e^j \leq e^{j^{[i]}} [j - j^{[i]} + 1], \quad (22)$$

where  $j \in \{ \xi_{g,cn}, \xi_{g,dn}, \xi_{l,k_m}^{sup}, \xi_{l,k_m}^{sub}, \xi_{p,k_m} \}$ . Hence, the constraints (21d), (21g), (21j), (21m) and (21p) can be rewritten as

$$S'_{g,dn} + I_{g,n}^{tot'} + \sigma_n^2 \leq e^{\xi_{g,cn}^{[i]}} [\xi_{g,cn} - \xi_{g,cn}^{[i]} + 1] \quad (23a)$$

$$I_{g,n}^{tot'} + \sigma_n^2 \leq e^{\xi_{g,dn}^{[i]}} [\xi_{g,dn} - \xi_{g,dn}^{[i]} + 1] \quad (23b)$$

$$S'_{l,ck_m} + S'_{l,pk_m} + I_{l,k_m}^{tot'} + \sigma_n^2 \leq e^{\xi_{l,k_m}^{sup [i]}} [\xi_{l,k_m}^{sup} - \xi_{l,k_m}^{sup [i]} + 1] \quad (23c)$$

$$S'_{l,pk_m} + I_{l,k_m}^{tot'} + \sigma_n^2 \leq e^{\xi_{l,k_m}^{sub [i]}} [\xi_{l,k_m}^{sub} - \xi_{l,k_m}^{sub [i]} + 1] \quad (23d)$$

$$I_{l,k_m}^{tot'} + \sigma_n^2 \leq e^{\xi_{p,k_m}^{[i]}} [\xi_{p,k_m} - \xi_{p,k_m}^{[i]} + 1]. \quad (23e)$$

Rank-one implies that there is only one nonzero eigenvalue, hence, the nonconvex constraints (17k) and (17l) can be reexpressed as

$$\text{tr}(\mathbf{F}_{g,c}) - \lambda_{\max}(\mathbf{F}_{g,c}) = 0, \quad \text{tr}(\mathbf{F}_{g,d}) - \lambda_{\max}(\mathbf{F}_{g,d}) = 0, \quad (24a)$$

$$\text{tr}(\mathbf{F}_{l,cm}) - \lambda_{\max}(\mathbf{F}_{l,cm}) = 0, \quad m \in \mathcal{M}, \quad (24b)$$

$$\text{tr}(\mathbf{F}_{l,pk_m}) - \lambda_{\max}(\mathbf{F}_{l,pk_m}) = 0, \quad k_m \in \mathcal{K}_m, \quad m \in \mathcal{M}. \quad (24c)$$

In order to include these constraints into the objective function (21a), we construct a penalty function and obtain

$$\begin{aligned} \max_{\substack{F, \alpha, c \\ \eta, \xi}} \quad & t - \beta \left\{ [\text{tr}(\mathbf{F}_{g,c}) - \lambda_{\max}(\mathbf{F}_{g,c})] + [\text{tr}(\mathbf{F}_{g,d}) - \lambda_{\max}(\mathbf{F}_{g,d})] \right. \\ & \left. + \sum_{m=1}^M [\text{tr}(\mathbf{F}_{l,cm}) - \lambda_{\max}(\mathbf{F}_{l,cm})] + \sum_{m=1}^M \sum_{k_m=1}^{K_m} [\text{tr}(\mathbf{F}_{l,pk_m}) - \lambda_{\max}(\mathbf{F}_{l,pk_m})] \right\}. \end{aligned} \quad (25)$$

To ensure that the penalty function is as small as possible, we choose the appropriate penalty factor  $\beta$ . Due to the existence of the penalty function, (25) is not concave. We utilize an iterative

approach to solve this problem [39]. Using  $\text{tr}(\mathbf{F}_{g,c}) - \lambda_{\max}(\mathbf{F}_{g,c})$  as an example, the following inequality can be derived

$$\begin{aligned} 0 &\leq \text{tr}(\mathbf{F}_{g,c}) - \lambda_{\max}(\mathbf{F}_{g,c}) \\ &\leq \text{tr}(\mathbf{F}_{g,c}) - (\mathbf{v}_{\max g,c}^{[i]})^H \mathbf{F}_{g,c} \mathbf{v}_{\max g,c}^{[i]}, \end{aligned} \quad (26)$$

where  $\mathbf{v}_{\max g,c}$  is a normalized eigenvector in association with the largest eigenvalue  $\lambda_{\max}(\mathbf{F}_{g,c})$ . Likewise, we define  $\mathbf{v}_{\max g,p}$  for  $\lambda_{\max}(\mathbf{F}_{g,d})$  and  $\mathbf{v}_{\max l,cm}$  for  $\lambda_{\max}(\mathbf{F}_{l,cm})$  as well as  $\mathbf{v}_{\max l,pk_m}$  for  $\lambda_{\max}(\mathbf{F}_{l,pk_m})$ 's associated eigenvectors. The iterative penalty function is represented by  $PF$

$$\begin{aligned} PF = & \beta \left\{ \left[ \text{tr}(\mathbf{F}_{g,c}) - (\mathbf{v}_{\max g,c}^{[i]})^H \mathbf{F}_{g,c} \mathbf{v}_{\max g,c}^{[i]} \right] + \left[ \text{tr}(\mathbf{F}_{g,d}) - (\mathbf{v}_{\max g,p}^{[i]})^H \mathbf{F}_{g,d} \mathbf{v}_{\max g,p}^{[i]} \right] \right. \\ & + \sum_{m=1}^M \left[ \text{tr}(\mathbf{F}_{l,cm}) - (\mathbf{v}_{\max l,cm}^{[i]})^H \mathbf{F}_{l,cm} \mathbf{v}_{\max l,cm}^{[i]} \right] \\ & \left. + \sum_{m=1}^M \sum_{k_m=1}^{K_m} \left[ \text{tr}(\mathbf{F}_{l,pk_m}) - (\mathbf{v}_{\max l,pk_m}^{[i]})^H \mathbf{F}_{l,pk_m} \mathbf{v}_{\max l,pk_m}^{[i]} \right] \right\}. \end{aligned} \quad (27)$$

Therefore, we solve the following subproblem:

$$\begin{aligned} \mathcal{P}_4 : \quad & \max_{\substack{F, \alpha, c \\ \eta, \xi}} \quad t - PF \\ \text{s.t.} \quad & (17b) - (17j), (17m), (21b), \\ & (21c), (21e), (21f), (21h), (21i), \\ & (21k), (21l), (21n), (21o), (23). \end{aligned} \quad (28a)$$

Problem  $\mathcal{P}_1$  has been transformed into convex problem and can be solved effectively using the CVX toolbox [40]. While solving  $\mathcal{P}_4$ , the results  $\{F^{[i]}, \xi^{[i]}\}$  from the  $i$ -th iteration are considered as constants. The existence of lower bounds, i.e., (26), ensures that the objective function converges. In other words, the rank-one constraints can be satisfied [39]. If the optimized symmetric matrices,  $\{\mathbf{F}_{g,c}, \mathbf{F}_{g,p}, \mathbf{F}_{l,cm}, \mathbf{F}_{l,pk} | k \in \mathcal{K}, m \in \mathcal{M}\}$ , are of rank one, then the optimal precoders of GEO and LEO satellites can be obtained by using eigenvalue decomposition. Alternatively, we use randomization to extract approximate solutions from the optimized symmetric matrices.

The steps of multilayer D-RSMA joint GEO-LEO precoders optimization scheme is summarized in Algorithm 1. The precoders are initialized by using Maximum Ratio Transmission (MRT) and Singular Value Decomposition (SVD) since they have been demonstrated to provide

---

**Algorithm 1:** SDP-based Optimization Scheme

---

```

1 Initialize:  $i \leftarrow 0$ ,  $t^{[i]} \leftarrow 0$ ,  $F^{[i]}$ ,  $\xi^{[i]}$ ;
2 repeat
3    $i \leftarrow i + 1$ ;
4   Solve problem (28) using  $F^{[i-1]}$ ,  $\xi^{[i-1]}$  and denote the optimal value of the objective
      function as  $\{t - PF\}^*$  and the optimal solutions as  $F^*$ ,  $\xi^*$ ;
5   Update  $\{t - PF\}^{[i]} \leftarrow \{t - PF\}^*$ ,  $F^{[i]} \leftarrow F^*$ ,  $\xi^{[i]} \leftarrow \xi^*$ ;
6 until  $|\{t - PF\}^{[i]} - \{t - PF\}^{[i-1]}| < \tau$ ;
7 for  $j \in \{\{g, c\}, \{g, p\}, \{l, cm\}, \{l, pk\} | k \in \mathcal{K}, m \in \mathcal{M}\}$  do
8   if  $\text{rank}(\mathbf{F}_j) = 1$  then
9     Use eigenvalue decomposition to  $\mathbf{F}_j$  and obtain the corresponding precoder
10  else
11    Use randomization to extract an approximate solution
12  end
13 end

```

---

good overall performance over a variety of channel realizations [16], [41]. The tolerance of the algorithm is denoted by  $\tau = 10^{-5}$ .

The convergence of Algorithm 1 is guaranteed since the solutions to the problem (28) at iteration  $i - 1$  is a feasible solution to the problem at iteration  $i$ . Therefore, the objective function  $t - PF$  rises monotonically and it is constrained above by the transmit power. At each iteration, the solution meets the KKT optimality criteria, which are the same as those of (16) at convergence [42]. The total number of iterations required for the convergence is approximated as  $\mathcal{O}(\log(\tau^{-1}))$ . At each iteration of the proposed SDP-based algorithm, the convex subproblem (28) is solved. The computational complexity of each iteration is mostly determined by the number of optimization variables, the number and size of Linear Matrix Inequality (LMI) constraints, and the size of Second Order Cone (SOC) constraints [43], [44]. The problem (28) has  $2N_{tg}^2 + (K + M)N_{tl}^2 + 2K + N$  design variables,  $6N + 9K + 1$  slack variables, and  $8N + 12K + M + 1$  LMI constraints of size 1. Therefore, the worst-case computational complexity is given by

$$\mathcal{O}\left(\log(\tau^{-1})(8N + 12K + M + 1)^{1/2} \cdot z \left[ z^2 + 2N_{tg}^2(N_{tg} + z) \right. \right. \\ \left. \left. + (K + M)N_{tl}^2(N_{tl} + z) + (2K + N)(1 + z) + (8N + 12K + M + 1)(1 + z) \right] \right), \quad (29)$$

where  $z = \mathcal{O}(2N_{tg}^2 + (K + M)N_{tl}^2 + 2K + N + 6N + 9K)$ .

## V. SIMULATION RESULTS

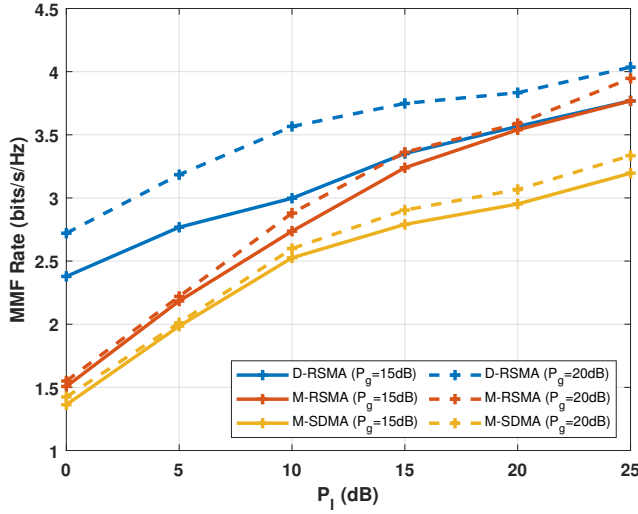
The performance of the proposed D-RSMA scheme is evaluated in this section. We assume all GEO and LEO satellites operate in the Ka-band [2], [3], [28]. The major simulation parameters are listed in Table II. Specifically, we assume the GEO satellite is equipped with  $N_{tg} = 4$  antennas, and  $N = 6$  multicasting GUs locate uniformly in coverage area. While two LEO satellites and each is deployed with  $N_{tl} = 3$  antennas, and LUs are uniformly distributed within LEO coverage. Because the noise power is normalized by  $\kappa T_{sys} B_w$  in (12) and (15), we denote unit noise variance, i.e.,  $\sigma_n^2 = 1$ ,  $\sigma_{k_m}^2 = 1$ ,  $\forall n \in \mathcal{N}$ ,  $\forall k_m \in \mathcal{K}$ ,  $m \in \mathcal{M}$ . We assume that GW has the perfect Channel State Information (CSI) of direct and interference links of the whole system. All MMF simulation results are obtained by averaging 100 channel realizations.

We compare the D-RSMA with two baseline multiple access schemes, namely, “M-RSMA” and “M-SDMA”. “M-RSMA” means multicasting is adopted at the GEO satellite and LEO satellites adopt 1-layer RSMA, while “M-SDMA” denotes multicasting is adopted at the GEO and LEO satellites implement SDMA.

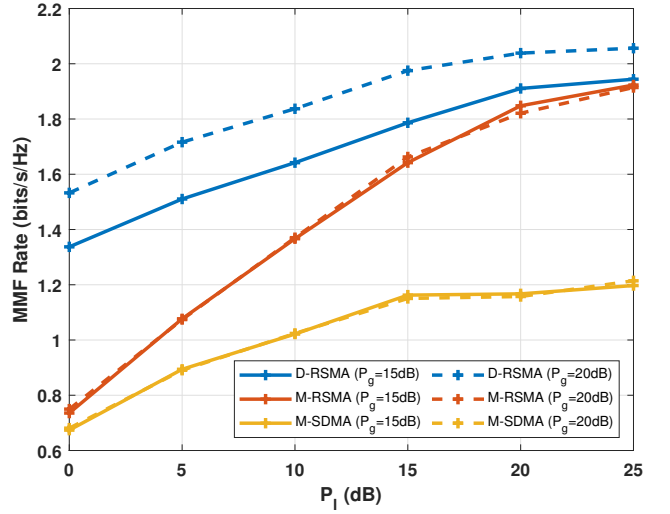
Fig. 3 compares the MMF performance of D-RSMA and baseline schemes under different system setups. Fig. 3(a) shows the MMF performance under 4 LUs deployments, each LEO satellite serves 2 LUs. Fig. 3(b) illustrates the MMF rate for overloaded scenario, i.e., 8 LUs in total, and 4 LUs are served by one satellite. From both subfigures, it can be seen that the MMF rates of all schemes rise and tend to saturate when the LEO transmit power budget  $P_l$  increases. D-RSMA achieves a clear MMF rate gain over all the other schemes in both subfigures. As  $P_l$  increases, the gap between D-RSMA and M-RSMA schemes gradually decreases and the two schemes converge when  $P_l$  is large enough. The reasons are as follows. The joint GEO-LEO beamforming optimization method is designed to attain the optimized MMF rates. When the power budget of LEO is relatively small, the system performance is restricted by the LUs since the SINRs of LUs are much lower than those of GUs. However, in the D-RSMA scheme, LUs messages are divided and parts of LUs’ data are encoded into common stream  $s_{g,c}$  transmitted

TABLE II  
SIMULATION PARAMETERS

| Parameter                  | GEO        | LEO        |
|----------------------------|------------|------------|
| Carrier frequency          | 20 GHz     |            |
| Bandwidth                  | 500 MHz    |            |
| User terminal antenna gain | 39.7 dBi   |            |
| Satellite height           | 35786 km   | 1200 km    |
| Antenna gain               | 58.5 dBi   | 30.5 dBi   |
| 3 dB bandwidth             | 0.4412 deg | 4.4127 deg |
| Rician factor              |            | 10 dB      |



(a)  $K = 4$ , 2 LUs under each LEO.



(b)  $K = 8$ , 4 LUs under each LEO.

Fig. 3. MMF rate versus  $P_l$  for different  $P_g$  and network loads.  $N_{tg} = 4$ ,  $N_{tl} = 3$ ,  $N = 6$ .

from the GEO satellite (thereby RSMA is distributedly implemented). This enables D-RSMA to utilize GEO power to transmit parts of LUs data, balancing the network load and managing the interference between two sub-networks. Due to the fixed GEO satellite transmit power budget  $P_g$ , the MMF rates of both D-RSMA and M-RSMA are constrained when  $P_l$  is sufficiently large. The benefit of the D-RSMA over the other strategies decreases as  $P_l$  increases. M-RSMA outperforms M-SDMA because we consider the LoS channels and the LUs channels are closely

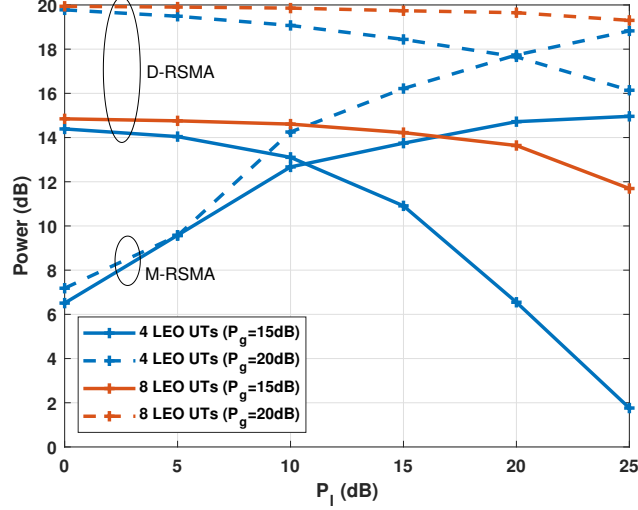


Fig. 4. GEO power allocation versus  $P_l$  for D-RSMA and M-RSMA under different  $P_g$  and network loads.  $N_{tg} = 4$ ,  $N_{tl} = 3$ ,  $N = 6$ .

aligned with each other. Compared to Fig. 3(a), the attained MMF rate in Fig. 3(b) decreases, while the benefit of distributed RSMA is enhanced further. The relative gain of “D-RSMA ( $P_g = 15$  dB)” over “M-RSMA ( $P_g = 15$  dB)” increases from 3.48% in Fig. 3(a) to 8.79% in Fig. 3(b) when  $P_l = 15$  dB. With more served LUs, the simultaneous inter-system and intra-system interference are severer. M-RSMA cannot manage the interference between sub-networks. However, by transmitting  $s_{g,c}$  from GEO, the interference can be coordinated and suppressed with the implementation of D-RSMA.

The influence of the GEO power budget is also investigated. From Fig. 3(a), the larger  $P_g$  leads to better MMF rate performance. Besides, D-RSMA benefits more from the increase in power budget since GEO can allocate more power to transmit the common message. Hence the overall max-min rate can be improved and the saturated rate when  $P_l$  is sufficiently large increases compared to that in the scenario with  $P_g = 15$  dB. The gap between “M-RSMA ( $P_g = 15$  dB)” and “M-RSMA ( $P_g = 20$  dB)” is larger when the power budget of LEO is large. This is because the system performance is restricted by the LUs when  $P_l$  is small, the increase of  $P_g$  does not help to increase the MMF rate of the system, while as the increase of  $P_l$ , the constraints of the system transform to the GUs due to the relatively low SINR, then the max-min rate can be improved resulting from the higher GEO power budget. When LEO satellites work in the overloaded deployment (Fig. 3(b)), only D-RSMA benefits from the increase of  $P_g$  since it can make use of the power from both sub-networks and manage the severer interference between

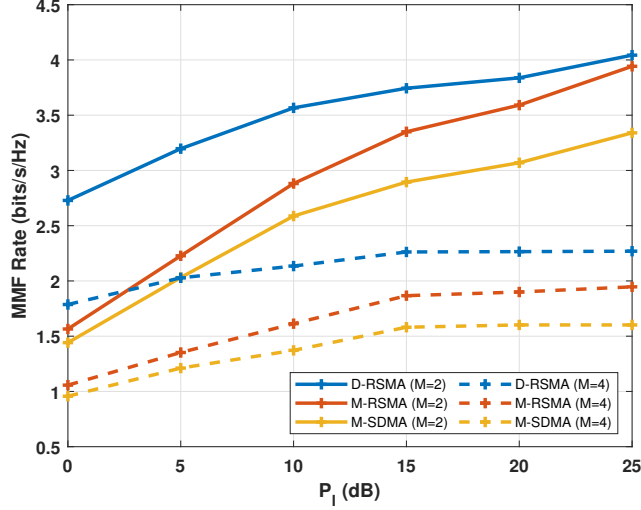


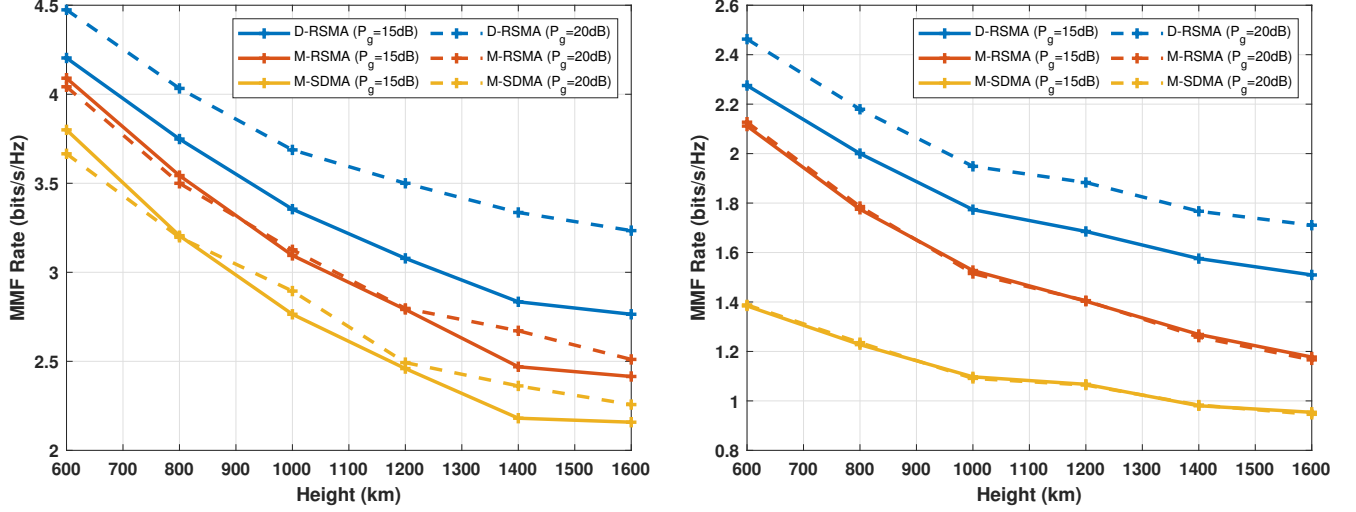
Fig. 5. MMF rate versus  $P_l$  with varied number of LEO satellites.  $N_{lg} = 4$ ,  $N_{tl} = 3$ ,  $N = 6$ ,  $P_g = 20$  dB.

GEO and LEO sub-networks. From Fig. 3, we can conclude that D-RSMA can well manage the interference and achieves MMF rate gain compared to M-RSMA and M-SDMA regardless of network loads, which guarantees user fairness. Alternatively, D-RSMA can utilize less power to achieve the same MMF performance.

We also investigate how power is allocated to the common stream or the multicasting stream for the GEO satellite in Fig. 4. The label “D-RSMA” denotes the power allocated to the common stream,  $s_{g,c}$ , in the D-RSMA scheme, and the label “M-RSMA” means how the GEO satellite utilizes power to transmit multicasting message in M-RSMA scheme. As the increase of LEO power budget, less power is allocated to the GEO common stream  $s_{g,c}$  in the D-RSMA method, while more power is utilized in the M-RSMA scheme. For D-RSMA scheme, more than 85% of the total GEO power is allocated to the  $s_{g,c}$  at  $P_l = 0$  dB to maintain the MMF rate of the system, regardless of network loads and GEO power constraints, which is inline with the observations from Fig. 3. When the number of LUs rises, more power is allocated to  $s_{g,c}$ , i.e., a larger portion of users private streams is encoded in the common stream. This is because each UT experiences severer multi-user interference in the overloaded scenario than in the underloaded case, as the transmission of  $s_{g,c}$  in D-RSMA, the amount of interference to be decoded at each UT is further enhanced.

The influence of the number of LEO satellites is illustrated in Fig. 5. 2 LUs are served by each LEO satellite. By increasing the number of LEO satellites and LUs, the MMF performances



(a)  $K = 4$ , 2 LUs under each LEO.(b)  $K = 8$ , 4 LUs under each LEO.Fig. 6. MMF rate versus LEO height for different  $P_g$  and network loads.  $N_{tg} = 4$ ,  $N_{tl} = 3$ ,  $N = 6$ ,  $P_l = 10$  dB.

of all schemes degrade, while D-RSMA still outperforms the other baseline approaches in all deployments. The relative gain of D-RSMA over M-RSMA increases from 11.74% in 2 LEO satellites deployment to 21.20% in 4 LEO satellites deployment when  $P_l = 15$  dB. Because, as the increase of LEO satellites and LUs, each UT suffers from severer inter-system and intra-system interference, without the transmission of  $s_{g,c}$ , M-RSMA cannot manage the interference coming from GUs and LUs that are not served by the same LEO. In comparison, D-RSMA is more robust to the number of co-existence LEO satellites and network load thanks to its ability to partially decode the interference and partially treat interference as noise.

The influence of LEO satellite height is investigated in Fig. 6 under varied network loads and GEO power constraints. The LEO power budget is fixed at  $P_l = 10$  dB. As the height of LEO satellites increases, the max-min rate decreases as expected in both subfigures. D-RSMA shows the best performance across all GEO power budgets and network loads. Without implementing distributed RSMA at GEO, the achievable rate in M-RSMA is limited by the worst-case UT, and its performance is mainly constrained by inter-system and intra-system interference. However, D-RSMA can well manage the interference and provide a performance gain compared to M-RSMA and M-SDMA. The loss of rate becomes more severe when there is a long transmit distance between LEO and LUs. In comparison, D-RSMA enhances the common rate of the worst-case UT (as equation (11)) by transmitting the common stream  $s_{g,c}$  to that UT. As the number of LUs

increases, the relative rate gain between “D-RSMA ( $P_g = 15$  dB)” and “M-RSMA ( $P_g = 15$  dB)” increases from 2.78% in Fig. 6(a) to 7.76% in Fig. 6(b) at 600 km. This is because with the number of LUs rising, multi-user interference grows and a larger proportion of user messages are transmitted by the common stream  $s_{g,c}$ . More interference can be decoded and subtracted from the received signal since D-RSMA enables LUs to partially decode the interference and partially treat interference as noise. Hence, D-RSMA enhances the MMF of the system.

## VI. CONCLUSION

To conclude, we investigate the co-existence of GEO-LEO multilayer network, where the RSMA is distributedly implemented (D-RSMA) to mitigate the interference and improve user fairness. The objective is to maximize the MMF rate by jointly optimizing the precoders of GEO and LEO satellites and the message split of each user subject to the power constraints at the satellites. We propose an SDP-based iterative optimization algorithm to solve the problem. We further show through numerical results that the proposed D-RSMA can well manage the interference and boost the MMF performance of the system. The influence of the LEO power budget, GEO power budget, the number of LUs and the number of LEO satellites is studied. We find that as the increase of GEO transmit power, or the number of serving LUs, the rate improvement of D-RSMA over other RSMA and SDMA baselines become more significant. Thanks to the transmission of GEO common stream, D-RSMA is more capable of managing inter-system and intra-system interference. Hence, we draw the conclusion that D-RSMA is superior to existing transmission schemes and has a great potential to improve the system performance of future communication networks.

## REFERENCES

- [1] 3GPP TR 22.822 V16.0.0, “3rd Generation Partnership Project; Technical Specification Group Services and System Aspects; Study on using Satellite Access in 5G; Stage 1(Release 16),” 3GPP, techreport, Jun. 2018.
- [2] 3GPP TR 38.821 V16.1.0, “3rd Generation Partnership Project; Technical Specification Group Radio Access Network; Solutions for NR to support non-terrestrial networks (NTN) (Release 16),” 3GPP, techreport, May 2021.
- [3] 3GPP TR 38.811 V15.4.0, “3rd Generation Partnership Project; Technical Specification Group Radio Access Network; Study on New Radio (NR) to support non-terrestrial networks (Release 15),” 3GPP, techreport, Sep. 2020.
- [4] B. Di, L. Song, Y. Li, and H. V. Poor, “Ultra-dense LEO: Integration of satellite access networks into 5G and beyond,” *IEEE Wireless Communications*, vol. 26, no. 2, pp. 62–69, April 2019.
- [5] Y. Liu, Y. Wang, J. Wang, L. You, W. Wang, and X. Gao, “Robust downlink precoding for LEO satellite systems with per-antenna power constraints,” *IEEE Transactions on Vehicular Technology*, vol. 71, no. 10, pp. 10 694–10 711, Oct 2022.

- [6] I. Leyva-Mayorga, B. Soret, and P. Popovski, "Inter-plane inter-satellite connectivity in dense LEO constellations," *IEEE Transactions on Wireless Communications*, vol. 20, no. 6, pp. 3430–3443, June 2021.
- [7] I. Leyva-Mayorga, B. Soret, M. Rper, D. Wbben, B. Matthiesen, A. Dekorsy, and P. Popovski, "LEO small-satellite constellations for 5G and beyond-5G communications," *IEEE Access*, vol. 8, pp. 184 955–184 964, 2020.
- [8] S. K. Sharma, S. Chatzinotas, and B. Ottersten, "In-line interference mitigation techniques for spectral coexistence of GEO and NGE0 satellites," *International Journal of Satellite Communications and Networking*, vol. 34, no. 1, pp. 11–39, 2016.
- [9] B. Li, Z. Fei, C. Zhou, and Y. Zhang, "Physical-layer security in space information networks: A survey," *IEEE Internet of Things Journal*, vol. 7, no. 1, pp. 33–52, Jan 2020.
- [10] C.-S. Park, C.-G. Kang, Y.-S. Choi, and C.-H. Oh, "Interference analysis of geostationary satellite networks in the presence of moving non-geostationary satellites," in *2010 2nd International Conference on Information Technology Convergence and Services*, Aug 2010, pp. 1–5.
- [11] C. Wang, D. Bian, S. Shi, J. Xu, and G. Zhang, "A novel cognitive satellite network with GEO and LEO broadband systems in the downlink case," *IEEE Access*, vol. 6, pp. 25 987–26 000, 2018.
- [12] R. Li, P. Gu, and C. Hua, "Optimal beam power control for co-existing multibeam GEO and LEO satellite system," in *2019 11th International Conference on Wireless Communications and Signal Processing (WCSP)*, Oct 2019, pp. 1–6.
- [13] P. Gu, R. Li, C. Hua, and R. Tafazolli, "Dynamic cooperative spectrum sharing in a multi-beam LEO-GEO co-existing satellite system," *IEEE Transactions on Wireless Communications*, vol. 21, no. 2, pp. 1170–1182, Feb 2022.
- [14] H. Joudeh and B. Clerckx, "Robust transmission in downlink multiuser MISO systems: A rate-splitting approach," *IEEE Trans. Signal Processing*, vol. 64, no. 23, pp. 6227–6242, 2016.
- [15] B. Clerckx, Y. Mao, R. Schober, and H. V. Poor, "Rate-splitting unifying SDMA, OMA, NOMA, and multicasting in MISO broadcast channel: A simple two-user rate analysis," *IEEE Wireless Communications Letters*, vol. 9, no. 3, pp. 349–353, March 2020.
- [16] Y. Mao, B. Clerckx, and V. O. Li, "Rate-splitting multiple access for downlink communication systems: Bridging, generalizing, and outperforming SDMA and NOMA," *Journal on Wireless Communications and Networking*, no. 133 (2018), 2018.
- [17] Y. Mao, O. Dizdar, B. Clerckx, R. Schober, P. Popovski, and H. V. Poor, "Rate-splitting multiple access: Fundamentals, survey, and future research trends," *IEEE Communications Surveys and Tutorials*, vol. 24, no. 4, pp. 2073–2126, Fourthquarter 2022.
- [18] A. Zappone, B. Matthiesen, and E. A. Jorswieck, "Energy efficiency in MIMO underlay and overlay device-to-device communications and cognitive radio systems," *IEEE Transactions on Signal Processing*, vol. 65, no. 4, pp. 1026–1041, Feb 2017.
- [19] Y. Mao, B. Clerckx, and V. O. Li, "Energy efficiency of rate-splitting multiple access, and performance benefits over SDMA and NOMA," in *2018 15th International Symposium on Wireless Communication Systems (ISWCS)*, 2018, pp. 1–5.
- [20] Y. Mao, B. Clerckx, J. Zhang, V. O. K. Li, and M. A. Arafah, "Max-min fairness of K-user cooperative rate-splitting in MISO broadcast channel with user relaying," *IEEE Transactions on Wireless Communications*, vol. 19, no. 10, pp. 6362–6376, 2020.
- [21] Y. Xu, Y. Mao, O. Dizdar, and B. Clerckx, "Max-min fairness of rate-splitting multiple access with finite blocklength communications," *IEEE Transactions on Vehicular Technology*, vol. 72, no. 5, pp. 6816–6821, May 2023.
- [22] H. Joudeh and B. Clerckx, "Rate-splitting for max-min fair multigroup multicast beamforming in overloaded systems," *IEEE Transactions on Wireless Communications*, vol. 16, no. 11, pp. 7276–7289, Nov 2017.
- [23] J. Xu, O. Dizdar, and B. Clerckx, "Rate-splitting multiple access for short-packet uplink communications: A finite blocklength analysis," *IEEE Communications Letters*, vol. 27, no. 2, pp. 517–521, Feb 2023.

- [24] O. Dizdar, Y. Mao, Y. Xu, P. Zhu, and B. Clerckx, "Rate-splitting multiple access for enhanced URLLC and eMBB in 6G: Invited paper," in *2021 17th International Symposium on Wireless Communication Systems (ISWCS)*, 2021, pp. 1–6.
- [25] Y. Liu, B. Clerckx, and P. Popovski, "Network slicing for eMBB, URLLC, and mMTC: An uplink rate-splitting multiple access approach," 2022. [Online]. Available: <https://arxiv.org/pdf/2208.10841.pdf>
- [26] Y. Xu, Y. Mao, O. Dizdar, and B. Clerckx, "Rate-splitting multiple access with finite blocklength for short-packet and low-latency downlink communications," *IEEE Transactions on Vehicular Technology*, vol. 71, no. 11, pp. 12 333–12 337, Nov 2022.
- [27] M. Caus, A. Pastore, M. Navarro, T. Ramirez, C. Mosquera, N. Noels, N. Alagha, and A. I. Perez-Neira, "Exploratory analysis of superposition coding and rate splitting for multibeam satellite systems," in *2018 15th International Symposium on Wireless Communication Systems (ISWCS)*, Aug 2018, pp. 1–5.
- [28] L. Yin and B. Clerckx, "Rate-splitting multiple access for multigroup multicast and multibeam satellite systems," *IEEE Transactions on Communications*, vol. 69, no. 2, pp. 976–990, Feb 2021.
- [29] —, "Rate-splitting multiple access for satellite-terrestrial integrated networks: Benefits of coordination and cooperation," *IEEE Transactions on Wireless Communications*, vol. 22, no. 1, pp. 317–332, Jan 2023.
- [30] Z. Lin, M. Lin, T. de Cola, J.-B. Wang, W.-P. Zhu, and J. Cheng, "Supporting IoT with rate-splitting multiple access in satellite and aerial-integrated networks," *IEEE Internet of Things Journal*, vol. 8, no. 14, pp. 11 123–11 134, July 2021.
- [31] V. Joroughi, M. . Vzquez, and A. I. Prez-Neira, "Generalized multicast multibeam precoding for satellite communications," *IEEE Transactions on Wireless Communications*, vol. 16, no. 2, pp. 952–966, Feb 2017.
- [32] G. Zheng, S. Chatzinotas, and B. Ottersten, "Generic optimization of linear precoding in multibeam satellite systems," *IEEE Transactions on Wireless Communications*, vol. 11, no. 6, pp. 2308–2320, June 2012.
- [33] K.-X. Li, L. You, J. Wang, X. Gao, C. G. Tsinos, S. Chatzinotas, and B. Ottersten, "Downlink transmit design for massive MIMO LEO satellite communications," *IEEE Transactions on Communications*, vol. 70, no. 2, pp. 1014–1028, Feb 2022.
- [34] L. You, K.-X. Li, J. Wang, X. Gao, X.-G. Xia, and B. Ottersten, "Massive MIMO transmission for LEO satellite communications," *IEEE Journal on Selected Areas in Communications*, vol. 38, no. 8, pp. 1851–1865, Aug 2020.
- [35] F. Fontan, M. Vazquez-Castro, C. Cabado, J. Garcia, and E. Kubista, "Statistical modeling of the lms channel," *IEEE Transactions on Vehicular Technology*, vol. 50, no. 6, pp. 1549–1567, Nov 2001.
- [36] A. V. Bagrov, V. A. Leonov, A. S. Mitkin, A. F. Nasyrov, A. D. Ponomarenko, K. M. Pichkhadze, and V. K. Sysoev, "Single-satellite global positioning system," *Acta Astronautica*, vol. 117, pp. 332–337, 2015. [Online]. Available: <https://www.sciencedirect.com/science/article/pii/S0094576515003343>
- [37] L. You, X. Qiang, C. G. Tsinos, F. Liu, W. Wang, X. Gao, and B. Ottersten, "Beam squint-aware integrated sensing and communications for hybrid massive MIMO LEO satellite systems," *IEEE Journal on Selected Areas in Communications*, vol. 40, no. 10, pp. 2994–3009, Oct 2022.
- [38] L. You, K.-X. Li, J. Wang, X. Gao, X.-G. Xia, and B. Ottersten, "LEO satellite communications with massive MIMO," in *ICC 2020 - 2020 IEEE International Conference on Communications (ICC)*, June 2020, pp. 1–6.
- [39] J. Chu, X. Chen, C. Zhong, and Z. Zhang, "Robust design for NOMA-based multibeam LEO satellite internet of things," *IEEE Internet of Things Journal*, vol. 8, no. 3, pp. 1959–1970, Feb 2021.
- [40] M. Grant, S. Boyd, and Y. Ye, "CVX: Matlab software for disciplined convex programming," 2008.
- [41] H. Joudeh and B. Clerckx, "Sum-rate maximization for linearly precoded downlink multiuser MISO systems with partial CSIT: A rate-splitting approach," *IEEE Transactions on Communications*, vol. 64, no. 11, pp. 4847–4861, 2016.
- [42] B. R. Marks and G. P. Wright, "A general inner approximation algorithm for nonconvex mathematical programs," *Operations Research*, vol. 26, no. 4, pp. 681–683, 1978. [Online]. Available: <http://www.jstor.org/stable/169728>

- [43] G. Zhou, C. Pan, H. Ren, K. Wang, and A. Nallanathan, "A framework of robust transmission design for IRS-aided MISO communications with imperfect cascaded channels," *IEEE Transactions on Signal Processing*, vol. 68, pp. 5092–5106, 2020.
- [44] A. Ben-Tal and A. Nemirovski, *Lectures on modern convex optimization: analysis, algorithms, and engineering applications*. SIAM, 2001.